

MVMR: Evaluating Natural Language Video Localization Bias over Multiple Reliable Videos Pool

Nakyeong Yang¹, Minsung Kim¹, Seunghyun Yoon², Joongbo Shin³, Kyomin Jung¹

¹Seoul National University, ²Adobe Research, ³LG AI Research
{yny0506, kms0805, kjung}@snu.ac.kr, syoon@adobe.com, jb.shin@lgresearch.ai

Abstract

With the explosion of multimedia content in recent years, natural language video localization, which focuses on detecting video moment that matches a given natural language query, has become a critical problem. However, none of the previous research explores localizing a moment from a large corpus where multiple positive and negative videos exist. In this paper, we propose an **MVMR** (Massive Videos Moment Retrieval) task, which aims to localize video frames from a massive set of videos given a text query. For this task, we suggest methods for constructing datasets by employing similarity filtering on the existing video localization datasets and introduce three MVMR datasets. Specifically, we employ embedding-based text similarity matching and video-language grounding techniques to calculate the relevance score between a target query and videos to define positive and negative sets. For the proposed MVMR task, we further develop a strong model, Reliable Mutual Matching Network (RMMN), which employs a contrastive learning scheme that selectively filters the reliable and informative negatives leading the model more robust on the MVMR task. Experimental results on the introduced datasets reveal that existing NLVL models are easily distracted by negative video frames, whereas our model shows significant performance.

1 Introduction

Enabled by the increased accessibility of video-sharing platforms along with the advancement of networking and storage technology, a vast number of new content is available on the web daily. With this huge number of contents, searching for video moments suitable for desired information has emerged as an essential problem (Anne Hendricks et al. 2017; Gao et al. 2017).

Researchers have studied this area as a natural language video localization (NLVL), which aims to detect a specific moment in a video that matches a given text query (Zhang et al. 2020b,a; Nan et al. 2021; Gao and Xu 2021; Liu et al. 2021; Wang et al. 2022). This line of research narrows down the task to an unpractical setting by targeting the search over a single video; thus, it bears limitations in retrieving relevant information over whole media pools.

Therefore, video corpus moment retrieval (VCMR) task that retrieves the correct positive moment among numerous negative videos has emerged (Escorcia et al. 2019; Lei



Figure 1: Massive Videos Moment Retrieval. MVMR searches among massive videos with multiple positive and negative videos considering the practical use case. If an NLVL model is not trained considering the MVMR setting, it may undergo a Type 1 error since it is not robust to distractors (videos).

et al. 2020). Nonetheless, the VCMR task also has limitations since it supposes that each natural language query is associated with only one positive video. This assumption diverges from the realistic setting of video moment search where multiple positive videos exist in whole media collections. For example, when a user intends to acquire knowledge on “How to use ChatGPT” and conducts a search for it on a video-sharing platform, a multitude of video moments should emerge that meet the user’s requirement. In addition, the existing VCMR studies have not considered the possibility that negative videos set contains false-negative videos when constructing video retrieval pools for a specific query. This is because they have converted NLVL datasets assuming that only the golden video mapped to a target query as positive and categorized all other videos as negative. Consequently, evaluating the performance of video moment search models using an existing VCMR framework may lead to unreliable results. In the case of TACoS test dataset, it is noteworthy that the number of videos with queries exactly matching the text “The person gets out a knife.” amounts to 15, constituting 60% of the entire dataset. When considering a broader matching encompassing semantic similarities, more videos will be included as false negatives.

To bridge these gaps, we propose an **MVMR** (Massive Videos Moment Retrieval) task, which expands the search coverage to a massive video set that can contain any number of positive videos as shown in Figure 1. Specifically, given a specific query q with a positive video set $V_q^+ = \{v_1^+, \dots, v_k^+\}$ and a negative video set $V_q^- = \{v_1^-, \dots, v_{n-k}^-\}$, the MVMR task aims to detect temporal moments in the positive videos V_q^+ that matches the query from a massive video set $V_q^{+,-} = \{v_1^+, \dots, v_k^+, v_1^-, \dots, v_{n-k}^-\}$.

Furthermore, we propose novel methods to construct an MVMR dataset by leveraging publicly available NLVL datasets (Gao et al. 2017; Krishna et al. 2017; Regneri et al. 2013). A critical challenge in converting an NLVL dataset into an MVMR dataset lies in accurately defining positive and negative videos for each query based solely on the information available in the dataset. To address this challenge, we employ a semantic text embedding model and a video captioning evaluation model to secure reliable MVMR positive and negative videos. Specifically, we examine the similarity between a target query and all videos in an NLVL dataset using these models. To this end, we construct three MVMR datasets, and we confirm that two samples of the introduced datasets contain only 1.5% and 0.2% falsely defined candidates, showing that our approach successfully creates a practical benchmark dataset from human evaluation.

The key aspect of solving the MVMR task is distinguishing positives from negative videos. To tackle the MVMR task, we introduce a strong model, Reliable Mutual Matching Network (RMMN), which accomplishes the key challenge of the MVMR task by mutually matching a query representation with positive video moment representations while increasing the distinction from negative ones. Specifically, RMMN identifies and excludes false and easy negatives to derive reliable and informative negative samples for a cross-directional contrastive learning scheme.

We demonstrate the performance of robust baseline models, including a state-of-the-art NLVL model and question-answering models, to compare with our model in the new scenario (MVMR). The experimental results show that the performance of baseline models degrades on the new task. For example, the state-of-the-art model, MMN, shows average 29.7% degradation on R@1(IOU0.5) for all MVMR datasets, revealing the difficulty of the MVMR task. On the other hand, our RMMN outperforms baseline models significantly in the MVMR setting, and reveals that our model mutually matches a query feature with positive video moment features while increasing the distinction from negative ones effectively.

2 Related Works

2.1 Natural Language Video Localization

The NLVL aims to detect a positive moment in a video that matches a given text query. The NLVL task has been explored extensively, with numerous effective methods emerging over time (Zhang et al. 2020b; Nan et al. 2021; Gao and Xu 2021; Liu et al. 2021; Wang et al. 2022). Some novel approaches have regarded the problem as question-answering

(QA) tasks (Wang and Jiang 2016; Seo et al. 2018; Joshi et al. 2020), by leveraging a QA model to encode a multi-modal representation and then predicting the frames that correspond to the start and end of the moment that match a query (Ghosh et al. 2019; Zhang et al. 2020a).

VCMR is an extension of the NLVL, where the task is to retrieve a moment from multiple videos for a given query. Escorcia et al. (2019) uses an existing NLVL dataset and extends it to the VCMR setting. Lei et al. (2020) proposes a new dataset for VCMR called TV show Retrieval (TVR). This dataset consists of videos, subtitles, and queries from multiple TV shows. However, these existing VCMR datasets do not account for the possibility that there may be many different moments corresponding to a single query.

2.2 Negative Samples in Contrastive Learning

Contrastive learning aims to congregate positive samples and disseminate negative samples within the feature space (Hadsell, Chopra, and LeCun 2006; Khosla et al. 2021). It has been recognized in various domains (Chen et al. 2020; Gao, Yao, and Chen 2022), including the vision-language area (Radford et al. 2021). Likewise, the NLVL task has revealed impressive results by applying contrastive learning between a query and a video moment (Wang et al. 2022).

The challenge in contrastive learning is deriving informative negatives from vast samples. Zhou et al. (2022) has focused on effective negative sampling, particularly in document retrieval. With a given query q , this task aims to bring relevant documents D^+ closer while pushing irrelevant documents D^- further from the query representation. Under the observation that overly similar (false-negative) or highly dissimilar (easy-negative) negative samples to a given query inhibit effective learning, Zhou et al. (2022) has achieved significant performance enhancement by modulating the sampling probability contingent on the difficulty level of the negative samples.

3 Problem Definition

We evaluate NLVL models using the MVMR dataset constructed with the k positive sample videos and the $n-k$ negative sample videos for each query. Given a positive video set $V_q^+ = \{v_1^+, \dots, v_k^+\}$ and a negative video set $V_q^- = \{v_1^-, \dots, v_{n-k}^-\}$, the MVMR task aims to localize a temporal moment (x_s^v, x_e^v) of a specific video v that matches the query from massive video set $V_q^{+,-} = \{v_1^+, \dots, v_k^+, v_1^-, \dots, v_{n-k}^-\}$. In the MVMR task, we aim to retrieve an optimal positive moment $(x_s^{v^+}, x_e^{v^+})^*$ that matches semantically with the text query q . We derive confidence scores for moments of the whole n massive videos using an NLVL model and select the moment with the highest score as a prediction.

4 MVMR Dataset Construction

In this section, we define the MVMR task and describe how to build the MVMR dataset using a public NLVL dataset. The process of building an MVMR dataset is as follows: (1) We calculate similarities between a target query and all videos set using a pre-trained text embedding model and

a video captioning evaluation model. (2) We add videos with the similarity higher than a positive threshold as positive candidates for the target text query. Similarly, we include videos with a similarity lower than a negative threshold as negative candidates. (3) We sample MVMR positive and MVMR negative videos for a target query from the pre-defined positive and negative candidate pools.

4.1 Query Similarity Filtering

This section describes how to calculate the similarity between a target query q and a video v using a pre-trained text embedding model, SimCSE (Gao, Yao, and Chen 2021), to decide which videos to filter out. NLVL datasets consist of videos set $V = \{v_1, \dots, v_{l_v}\}$ and corresponding queries set $Q_v = \{q_1^v, \dots, q_{l_q}^v\}$ for each video v , where l_v and l_q is the number of videos and text queries included in the video, respectively. Since text queries in a video provide a description of the video, we use the queries to obtain semantic information about the video. Specifically, we calculate the similarity between a target query and video’s queries. We first obtain an embedding e_q of the target text query q using SimCSE. We also derive query embeddings set $E_v = \{e_{q_1^v}, \dots, e_{q_{l_q}^v}\}$ by embedding all video text queries Q_v . We calculate cosine similarity between e_q and $e_{q_i^v}$ to obtain the similarity $s_{te}(q, q_i^v)$. And then, we find the most similar one among the video’s queries and define the similarity of it as the similarity between q and v as follows:

$$s_{te}(q, v) = \max(\{s_{te}(q, q_1^v), \dots, s_{te}(q, q_{l_q}^v)\}) \quad (1)$$

Even if there is only one similar query in a video, it can be considered a positive video for the target query. Hence, using the highest value query similarity as the video’s similarity is reasonable. Each query assigned to a video is a dataset-specific text description, which has a similar textual form. Therefore, query similarity is appropriate to filter out false-negative videos.

4.2 Query-video Similarity Filtering

Queries provide standardized information about a video, but may contain insufficient information of a specific video. Therefore, we use a semantic matching score between a query and a video and filter positive and negative videos through it. We use EMscore (Shi et al. 2022), a zero-shot video captioning evaluation model, to calculate the query-video similarity s_{tv} and use it for an additional filtering on videos primarily filtered through the query similarity s_{te} .

4.3 False-negative Videos Filtering

This section describes how to construct MVMR positive and MVMR negative video sets by filtering false-negative videos using the calculated query-video similarities, s_{te} and s_{tv} .

MVMR positive candidates are constructed by (1) primarily filtering out videos with $s_{te}(q, v) < t_{te}^+$ and (2) removing videos that have lower similarity than the mean s_{tv} of all golden positive query-video pairs (q, v^*) for all queries as follows:

$$V^{c,+}(q) = \{v | s_{te}(q, v) \geq t_{te}^+ \cap s_{tv}(q, v) \geq \mu_{s_{tv}}^*\} \quad (2)$$

where $\mu_{s_{tv}}^*$ is the mean similarity of $s_{tv}(q, v^*)$ for all queries. We construct final MVMR positives by randomly sampling k videos from this set of positive candidates.

MVMR negative candidates are defined by (1) filtering out videos with $s_{te}(q, v) > t_{te}^-$ and (2) excluding videos that have higher similarity than the mean s_{tv} of query-video pairs (q, v^-) that is primarily filtered as negatives using s_{te} as follows:

$$V_{te}^{c,-}(q) = \{v | s_{te}(q, v) \leq t_{te}^-, \forall v \in V$$

$$\bar{\mu}_{s_{tv}} = \frac{1}{N} \sum_{i=1}^N s_{tv}(q, v_i), \forall (q, v_i) \in V_{te}^{c,-} \quad (3)$$

$$V^{c,-}(q) = \{v | s_{tv}(q, v) \leq \bar{\mu}_{s_{tv}}, \forall v \in V_{te}^{c,-}(q)$$

where N is the number of video samples in $V_{te}^{c,-}$. We also construct final MVMR negatives by randomly sampling $(n - k)$ videos from this set of negative candidates. In this process, a total of n video retrieval pools $V_q^{+,-} = \{v_1^+, \dots, v_k^+, v_1^-, \dots, v_{n-k}^-\}$ are obtained for each query.

5 Reliable Negatives Selection in Training

A key challenge in solving the MVMR task is distinguishing positives from multiple negative distractors. MMN (Wang et al. 2022) has used contrastive learning to represent negative samples effectively, showing the remarkable NLVL performance. This training scheme can also significantly improve the performance of the MVMR task. However, MMN disregards out-video false-negatives since it treats all randomly selected in-batch samples as negatives. In addition, it does not consider easily distinguishable negatives during training process. To enhance MVMR performance, it is crucial to filter out these uninformative negatives. In this chapter, we introduce the Reliable Mutual Matching Network (RMMN) which excludes false or easily distinguishable negatives from the training process.

5.1 Reliable True-negatives Filtering

The reliable true-negative filtering in the training process is similar to the query similarity filtering of the MVMR dataset construction described in Section 4.1. We pre-construct a query-video similarity matrix using the SimCSE score, and define samples with a similarity lower than t_{tr} as a reliable true-negative samples:

$$V_{tr}^-(q) = \{v | s_{te}(q, v) < t_{tr}\}, \forall v \in V \quad (4)$$

We use only the filtered true-negative samples as negative samples for contrastive learning.

5.2 Reliable Hard-negatives Filtering

Even if a model is trained using negative samples, it may not learn the correct representation since it can be distracted by easy-negatives and false-negatives. Inspired by recent progress in using hard-negative sampling for the document retrieval task (Zhou et al. 2022), in this work, we propose a

strong method to improve the MVMR performance, ‘Cross-directional Query-video Matching Ambiguous Negatives Sampling (CM-ANS)’, which is a hard negative sampling method considering the cross-directional query-to-video and video-to-query hard-negatives. we can categorize negatives using the relevance score between a target query and negative moments as follows: (1) Negatives that are clearly irrelevant and have low relevance scores should be sampled less frequently (Easy-negative); (2) Negatives that are highly relevant and have high relevance scores should also be sampled less frequently (False-negative); (3) Negatives that are uncertain and have relevance scores similar to true-positives should be sampled more frequently, since they provide useful information (Hard-negative). Therefore, we define the negative moments sampling distribution as follows:

$$p'(m|q) \propto \exp(-a(r(q, m) - \bar{r}(q, m^+) - b)^2), \quad \forall m \in M_q^- \quad (5)$$

where $r(q, m)$ is a relevance score between a query and a moment calculated using the already trained video moment retrieval model, and $\bar{r}(q, m^+)$ is a mean relevance score for all positive moments. M_q^- is the negative moment candidates for a query q . a is a hyper-parameter to control the density of the distribution. Likewise, we can define the negative queries sampling probability distribution as follows:

$$p'(q|m) \propto \exp(-a(r(q, m) - \bar{r}(q^+, m) - b)^2), \quad \forall q \in Q_m^- \quad (6)$$

where Q_m^- means the negative query candidates for each video moment. Since there are vast moments even in one video, the sampling process from this distribution considering all moments is excessively expensive. Therefore, we reformulate the formula to reduce the computational cost by converting the moment m to the video v as follows:

$$\begin{aligned} r(q, v) &= \max(\{r(q, m_1), \dots, r(q, m_l)\}), \quad \forall m_i \in v \\ p'(v|q) &\propto \exp(-a(r(q, v) - \bar{r}(q, v^+) - b)^2), \quad \forall v \in V_q^- \end{aligned} \quad (7)$$

$p'(q|v)$ can be formulated similarly by calculating \bar{r} about positive queries for each video. We define the distributions for negatives, and train our model using contrastive learning by sampling hard-negatives from them. These distributions are used to train pre-trained models further to focus on learning representations of informative negatives.

5.3 Reliable Mutual Matching Network

This section describes a novel model, Reliable Mutual Matching Network (RMMN), that uses our negative sampling methods for solving the MVMR task. RMMN adopts a bi-encoder architecture with a late modality fusion by an inner product in the joint visual-text representational space following the baseline MMN. Adopting a bi-encoder structure is important since the MVMR aims to search on massive videos. Given a user query, we can efficiently search for moments with pre-calculated video moment representations by using bi-encoder structure.

Query and Video Encoders. We choose DistilBERT (Sanh et al. 2019) for the text query encoder following MMN

since it is a light-weighted efficient model showing significant performance. We calculate the representation of each query $f^q \in \mathbb{R}^d$ using the global average pooling over all token. We adopt the approach of encoding the input video as a 2D temporal moment feature map, inspired by 2D-TAN (Zhang et al. 2020b) and MMN. To achieve this, we segment the input video into video clips denoted as $\{c_i\}_{i=1}^{l_c/k}$, where each clip c_i consists of k frames. l_c means the total number of frames in the video. The clip-level representations are extracted using a pre-trained visual model (e.g., C3D). By sampling a fixed-length with a stride of $\frac{l_c}{k \cdot N}$, we obtain N clip-level features. These features are then passed through an FC layer to reduce the dimensionality, resulting in the features $\{f_i^v\}_{i=1}^N$, where $f_i^v \in \mathbb{R}^d$. Utilizing these features, we construct a 2D temporal moment feature map $F \in \mathbb{R}^{N \times N \times d}$ by employing max-pooling as the moment-level feature aggregation method following the baseline (Wang et al. 2022). Additionally, we generate a 2D feature map F' of the same size by passing F to 2D Convolution, allowing the representation of moment relations as employed in MMN.

Joint Visual-Text Space. Initially, we apply layer normalization to both the video moments and text features. Subsequently, we utilize a linear projection layer and a 1×1 convolution layer to project the text and video in the same embedding space, respectively. The projected features are then employed in two distinct representational spaces: the IoU space and the mutual matching space. These spaces serve as the basis for computing the binary cross-entropy loss and the contrastive learning loss, respectively.

Reliable Mutual Matching. We choose the binary cross entropy and contrastive learning loss to represent the video and text features. We train our RMMN following two steps: (1) the first training step using the two loss functions (binary cross entropy and contrastive learning loss) with only true-negatives by filtering out false-negatives described in Section 5.1; (2) the second training step using two loss functions with only hard-negatives by removing false-negatives and easy-negatives as Section 5.2.

To calculate the similarity between the text and video moment features projected in the IoU space, we compute the cosine similarity s^{iou} . To adjust the range of the final prediction, we multiply the cosine similarity by a factor of 10. This amplification results in the final prediction $p_i^{iou} = \sigma(10 \cdot s_i^{iou})$, where σ represents the sigmoid function. The binary cross-entropy loss is then calculated as follows:

$$L_{bce} = -\frac{1}{C} \sum_{i=1}^C (y_i \log p_i^{iou} + (1 - y_i) \log (1 - p_i^{iou})) \quad (8)$$

where p_i^{iou} is the confidence score of each moment, and C is the total number of valid candidates. We calculate L_{bce} not only for the positive samples but for the reliable negatives.

We use the cross-directional contrastive learning loss to effectively train the model using the negatives, where we select only informative negatives using the method described in Section 5.1 and 5.2. The mutual matching contrastive

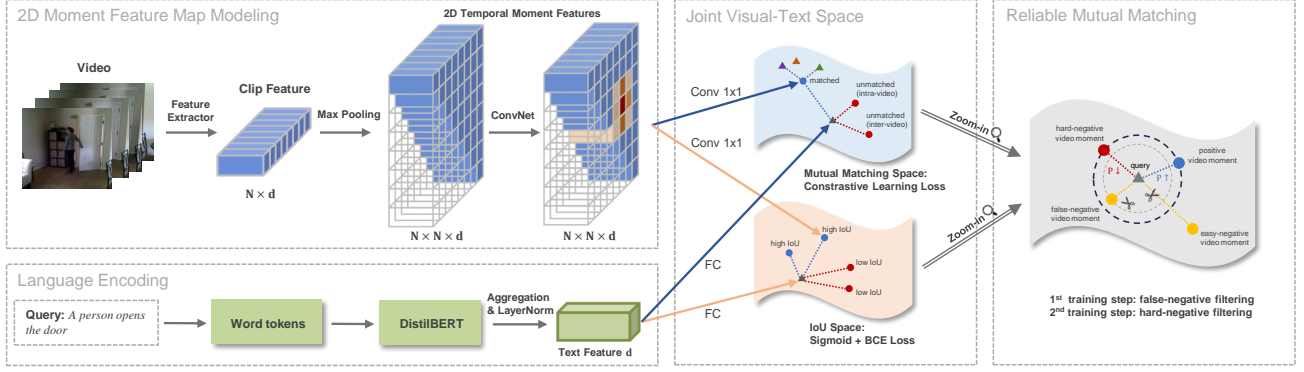


Figure 2: Reliable Mutual Matching Network. We apply true and hard negatives filtering for the MVMR task. The dots and triangles are the feature of moments and texts. The blue dash lines are matched moment-text pairs to be pulled in, while the red dash lines are negative samples of intra/inter-video to be pushed away. The yellow dash lines are unmatched moment-text pairs, but not to train by filtering out since they are uninformative negatives.

learning loss considering the negative samples selection process is as follows:

$$\begin{aligned}
 p^*(q_i|m) &= \frac{\exp((f_i^{qT} f^m - \psi)/\tau_m)}{\exp((f_i^{qT} f^m - \psi)/\tau_m) + \sum_{j \in \mathcal{I}_m^-} \exp(f_j^{qT} f^m/\tau_m)} \\
 p^*(m_i|q) &= \frac{\exp((f_i^{mT} f^q - \psi)/\tau_q)}{\exp((f_i^{mT} f^q - \psi)/\tau_q) + \sum_{j \in \mathcal{I}_q^-} \exp(f_j^{mT} f^q/\tau_q)} \\
 L_{rmm} &= -(\sum_{i=1}^N (\log p^*(i_m|q_i)) + \sum_{i=1}^N (\log p^*(i_q|m_i)))
 \end{aligned} \tag{9}$$

where q_i and m_i are corresponding positive query and moment for each moment and query, respectively. f^m and f^q are the moment and query features in joint visual-text space. τ_q and τ_m are temperatures. \mathcal{I}^- means the indices of informative negatives derived using negatives selection methods.

The final loss, denoted as L , is formulated as a linear combination of the binary cross-entropy loss and the reliable mutual matching loss. The matching score s , for a specific moment given the text query, is obtained by multiplying the iou score s^{iou} , with the reliable mutual matching score s^{rmm} . The reliable mutual matching score is calculated for the features in the mutual matching space the same as the iou score.

$$L = L_{bce} + \lambda L_{rmm}, \quad s = s^{iou} \cdot s^{rmm} \tag{10}$$

6 Experiments

6.1 NLVL Datasets

We construct the MVMR evaluation datasets (§4) using three widely-used NLVL datasets and name them $MVMR_{\{\text{DATASOURCE}\}}$. Each NLVL dataset consists of multiple videos with query-moment pairs. Charades-STA (Gao et al. 2017) is an extended dataset of action recognition and localization dataset Charades (Sigurdsson et al. 2016) for video moment retrieval. ActivityNet-Captions (Krishna et al. 2017) is constructed on ActivityNet v1.3 dataset (Heilbron et al. 2015), where included videos cover various complex human actions. TACoS (Regneri et al. 2013) includes videos selected from the MPII-Cooking dataset (Rohrbach

et al. 2012). It consists of various cooking activity annotations in the kitchen. The details of each NLVL dataset are shown in Appendix A.

6.2 MVMR Settings.

This section describes how to derive MVMR positive and negative candidates using SimCSE and EMScore in details.

SimCSE Filtering. For the query similarity filtering (§4.1 and §4.3), we use $t_{te}^+ = 0.9$ to derive MVMR positive candidates as a conservative threshold for constructing a reliable MVMR dataset. Indeed, if a threshold between 0.5 and 0.9 is chosen, query instances with lexical overlaps are derived, even if the meaning is completely shifted since the subject is different (e.g. "A man eats some food." vs "A girl eats some food."). To derive MVMR negative candidates, $t_{te}^- = 0.5$ was used since the cosine similarity regards two embeddings as highly correlated pair when the score is higher than 0.5.

EMScore Filtering. We set $\bar{\mu}_{stv}$ as the EMScore threshold to filter out false-negatives to construct MVMR candidates (§4.2 and §4.3). We calculate $\bar{\mu}_{stv}$ approximately by sampling a single negative video about each query to have computational efficiency.

6.3 MVMR Analysis.

We set a video retrieval pool as a total of n , containing at most k positive videos for each query. If the number of MVMR positive candidates derived for each query is less than k , we include all positive candidates as positive samples. Also, if the total number of MVMR positive candidates and MVMR negative candidates for a query is less than n , the query is excluded from the final MVMR dataset.

Datasets Statistic. We set the number of videos in the $MVMR_{\text{Charades-STA}}$ and the $MVMR_{\text{ActivityNet}}$ retrieval pools as $n = 50$, and the maximum number of positive moments per query k is set to 5. The former consists of 3,716 queries for 1,334 videos, and each query contains an average of 3.07 number of positive videos. The latter contains 16,941 queries for 4,885 videos, and each query includes an average of 1.11 number of positive videos. We set the num-

Dataset	Model	R@1 IOU0.3	R@1 IOU0.5	R@1 IOU0.7	R@5 IOU0.3	R@5 IOU0.5	R@5 IOU0.7	R@20 IOU0.3	R@20 IOU0.5	R@20 IOU0.7	R@50 IOU0.3	R@50 IOU0.5	R@50 IOU0.7
MVMR _{Charades-STA}	CET	3.96	2.96 (41.77)	2.02 (21.80)	15.34	11.79 (61.10)	6.97 (40.91)	39.85	32.21	19.91	59.58	50.54	33.88
	BET	4.57	2.99 (38.25)	1.94 (20.73)	14.26	10.98 (61.29)	7.00 (39.27)	31.05	25.11	16.55	45.88	37.86	26.08
	MMN	13.99	12.78 (47.18)	8.40 (27.47)	37.86	33.29 (83.71)	22.36 (56.96)	64.80	57.83	41.71	80.11	73.09	56.75
	RMMN [†]	<u>18.38</u>	<u>16.31</u> (47.55)	<u>10.76</u> (27.80)	43.86	39.05 (83.63)	<u>26.99</u> (58.28)	69.48	62.89	<u>46.39</u>	<u>82.88</u>	<u>76.08</u>	<u>60.28</u>
	RMMN	19.27	17.38 (48.06)	11.44 (27.53)	<u>43.54</u>	<u>39.02</u> (83.82)	27.91 (57.66)	<u>68.08</u>	<u>60.98</u>	46.39	82.99	76.29	60.76
MVMR _{ActivityNet}	CET	1.26 (63.68)	0.90 (46.52)	0.56 (27.81)	2.81 (83.23)	2.32 (72.84)	1.75 (58.34)	5.41	4.73	3.87	8.97	8.02	6.56
	BET	1.56 (62.82)	1.16 (44.84)	0.76 (26.73)	3.02 (84.97)	2.55 (74.74)	2.03 (60.27)	5.30	4.64	3.80	8.13	7.10	5.88
	MMN	13.82 (64.72)	10.71 (47.93)	6.93 (29.16)	31.54 (87.10)	25.04 (79.39)	16.55 (64.68)	54.79	44.50	30.62	73.08	62.09	<u>45.76</u>
	RMMN [†]	<u>16.46</u> (63.44)	<u>12.68</u> (47.17)	<u>7.87</u> (28.64)	<u>36.03</u> (86.07)	<u>28.47</u> (77.43)	<u>18.16</u> (62.06)	<u>57.91</u>	<u>46.52</u>	<u>31.12</u>	<u>73.82</u>	<u>62.12</u>	44.89
	RMMN	20.63 (64.25)	15.58 (47.82)	9.51 (28.52)	44.13 (86.34)	34.70 (78.40)	22.40 (63.45)	67.01	55.58	38.55	79.91	70.02	53.20
MVMR _{TACoS}	CET	8.95 (37.25)	5.79 (25.0)	3.89	26.18 (60.25)	18.88 (46.50)	12.17	54.84	42.53	23.70	-	-	-
	BET	8.22 (30.37)	5.30 (18.0)	2.97	29.46 (60.96)	14.84 (44.61)	8.32	55.67	39.76	21.51	-	-	-
	MMN	10.56 (39.20)	8.61 (26.27)	5.60	36.16 (62.11)	25.84 (47.42)	15.47	58.20	43.89	23.80	-	-	-
	RMMN [†]	13.43 (38.97)	<u>10.75</u> (27.62)	<u>6.76</u>	<u>36.45</u> (61.51)	<u>27.01</u> (47.46)	<u>15.28</u>	<u>58.30</u>	<u>44.38</u>	25.16	-	-	-
	RMMN	<u>13.24</u> (38.44)	10.75 (27.39)	7.30	39.22 (61.98)	29.68 (47.31)	16.50	60.05	44.77	<u>24.62</u>	-	-	-

Table 1: Results on MVMR datasets for RMMN and the baseline models. Bolded and under-lined results indicate the 1st and 2nd best performance, respectively. RMMN[†] is the model using only reliable true-negatives filtering (§5.1). RMMN uses both of two reliable negatives filtering method (§5.1 and §5.2). The values in parentheses are the results from the NLVL task. We train all the baselines as three trials and report the averaged NLVL and the MVMR scores.

ber of videos for the MVMR_{TACoS} and the maximum number of positive moments per query as 5 and 5, respectively, since TACoS test set contains only 25 videos. It includes of 2,055 queries for 25 videos, and each query contains an average of 2.24 number of positive videos. The summary of the MVMR datasets is shown in Appendix B.

Analysis on Dataset Filtering Methods. We visualize the scores derived using SimCSE and EMScore to verify the reliability of our MVMR datasets. Figure 3 displays SimCSE embeddings of all queries in each dataset, illustrating the similarity between all queries and a specific target query (left: “person turn a light on.”; right: “He is using a push mower to mow the grass.”). We use T-SNE to reduce the dimensionality of each query for displaying each query (dot).

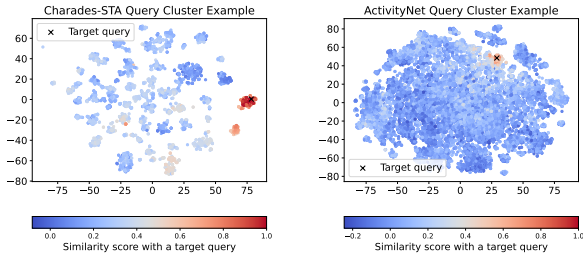


Figure 3: SimCSE Similarity Distribution

The figure reveals that queries exhibit well-defined clusters when setting 0.9 threshold for the Charades-STA and TACoS. The figure for the TACoS can also be found in Appendix C. Figure 4 presents histograms of the SimCSE similarity. The histograms indicate that Charades-STA and TACoS contain numerous text queries with high similarity, supporting the effectiveness of the query similarity filtering.

Figure 5 illustrates histograms representing the EMScore similarity between queries and videos that primarily filtered into positives and negatives using SimCSE. The red and blue histograms correspond to the EMScore distribution of positive and negative samples, respectively. For the ActivityNet, EMScore effectively distinguishes between positives

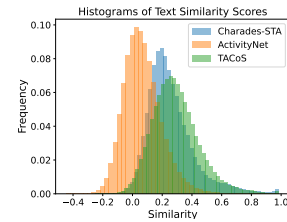


Figure 4: Histogram of SimCSE Similarity

and negatives. This success is attributed to that ActivityNet includes detailed queries and videos with diverse features.

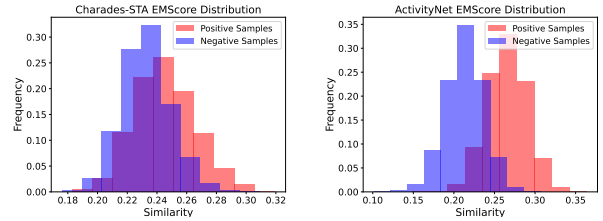


Figure 5: EMScore Similarity Distribution

According to the findings presented in this section, the filtering method’s efficacy varies depending on the dataset’s characteristics. Consequently, it is evident that a combination of two filtering methods (§4.1 and §4.2) should be employed in a complementary manner to ensure the construction of a reliable MVMR dataset.

Dataset Quality. This section verifies the quality by analyzing the three MVMR datasets. Appendix E shows examples of false-negative instances included in the constructed datasets as positive. In the case of Charades-STA dataset, it is evident that the appropriate videos for a target query “person opens a fridge door” are identified as positives. We also conduct a human evaluation on our MVMR datasets to reveal that our method build MVMR datasets effectively. We recruit crowd workers and let them examine 100 queries by classifying whether the query and paired video samples are relevant for each dataset. Overall, we analyze 4,900, 4,900, and 400 videos for Charades-STA, ActivityNet, and TACoS,

respectively, since each MVMR dataset consists of 49, 49, and 4 newly added positive and negative samples, except for the original golden positive video. From human evaluation, we confirm that the newly introduced dataset contains only 1.5%, 0.2%, and 3.5% falsely categorized videos for the three datasets, respectively. TACoS exhibits a relatively higher query-relevant video ratio than the other two datasets since its test set includes only 25 videos and consists of considerably similar cooking activities within the kitchen.

6.4 Baselines

We demonstrate three strong baseline models on constructed three MVMR evaluation datasets. We first select the state-of-the-art model of the NLVL tasks, MMN (Wang et al. 2022). As the MVMR task can be formulated as an open-domain question answering (QA) task, we further choose two types of QA models that employ a cross-encoder architecture (i.e., Cross-Encoder Transformer) and a dual-encoder architecture (i.e., Bi-Encoder Transformer), respectively. These architectures are widely adopted in existing NLVL tasks (Zhang et al. 2020b; Gao and Xu 2021) due to the closeness of the two tasks. The implementation details of baselines are shown in Appendix D.

MMN adopts a dual-modal encoding design to get video clip (moment) and text representations. MMN calculates the similarity between the encoded video clip and text representations to predict a matched moment. Furthermore, MMN uses the contrastive learning scheme to learn dense representational space. Cross-Encoder Transformer (CET) is a cross-modal encoding model implemented based on transformer encoder (Vaswani et al. 2017). It is designed to predict the start and end points of a video moment by calculating the score for each video clip. Bi-Encoder Transformer (BET) is a dual-modal encoding model which encodes text and video clip features independently. It is also designed to predict the start and end points of a video moment following (Lee et al. 2021). We localize a moment by calculating the similarity between the encoded video clip representations and the encoded start and end representations, respectively.

6.5 Experimental Settings

Implementation Details. We use standard off-the-shelf video feature extractors without any fine-tuning: VGG (Simonyan and Zisserman 2015) feature for Charades-STA; C3D (Tran et al. 2015) feature for ActivityNet and TACoS following (Wang et al. 2022). The reliable true-negatives filtering threshold is set as $t_{tr} = 0.9$. We choose the number of the CM-ANS samples to calculate $p'(q|v)$ as 100, 200, and 100 and $p'(v|q)$ as 50, 100, and 5 for Charades-STA, ActivityNet, and TACoS, respectively. In the hard-negative fine-tuning stage, the learning rates are degraded by multiplying 0.1. More detailed settings is shown in Appendix D.

Evaluation Metrics. Following previous setting (Gao et al. 2017) of the NLVL, we evaluate baselines by calculating Rank $n@m$. It is defined as the percentage of queries having at least one correctly retrieved moment, i.e. $\text{IoU} \geq m$, in the top- n derived moments. The existing NLVL studies have reported the results of $m \in \{0.3, 0.5, 0.7\}$ with

$n \in \{1, 5\}$ (Wang et al. 2022). But, since our MVMR setting aims to search for massive videos, it is insufficient to analyze the ability of models with previously designed metrics. Hence, we report the extended results as $m \in \{0.3, 0.5, 0.7\}$ with $n \in \{1, 5, 20, 50\}$ for Charades-STA and ActivityNet and $m \in \{0.3, 0.5, 0.7\}$ with $n \in \{1, 5, 20\}$ for TACoS. We use the same metrics in the previous study (Wang et al. 2022) to report the NLVL scores (parentheses).

6.6 MVMR Results

MVMR Performance. We evaluate the performance of RMMN and the baseline models on the introduced MVMR datasets. Table 1 shows that all the baseline models undergo significant performance degradation in the MVMR task. For example, MMN shows 47.18, 27.47 scores for $R@1(\text{IoU}0.5)$, $R@1(\text{IoU}0.7)$, respectively, on the $\text{NLVL}_{\text{Charades-STA}}$. However, it shows 12.78, 8.40 scores for the same metrics on the $\text{MVMR}_{\text{Charades-STA}}$. We reveal that RMMN outperforms all other baselines on MVMR task, and this suggests that our model correctly discriminates features of negative and positive videos. Experiments show that the models on Charades-STA and TACoS significantly improve performance from the true-negative filter since similar query overlap frequently exists in these datasets. However, the performance of ActivityNet is attributed to the hard-negative filter because it includes various and complex text queries. Our experimental findings also show that despite RMMN demonstrating comparable performance on NLVL task with other baselines, the model exhibits superior performance on MVMR task. These outcomes indicate that the current NLVL task performance alone is not enough to verify that a model is well-trained.

MVMR Performance with Video Retrieval Model. We also conduct MVMR experiments with a video retrieval model, PRMR model (Dong et al. 2022) as Table 2. We construct a pipeline to filter top-5 logit videos from our MVMR retrieval pool by using PRMR model and solve MVMR task. We use the publicly deployed fine-tuned PRMR model on Charades-STA and ActivityNet datasets. These experiments prove that video retrieval models are helpful to increase MVMR performance, and RMMN still shows superior performance than MMN in this pipeline.

Model	$R@1 \text{IoU}0.3$	$R@1 \text{IoU}0.5$	$R@5 \text{IoU}0.3$	$R@5 \text{IoU}0.5$
MMN _{Charades-STA}	32.15	27.10	65.97	57.66
RMMN _{Charades-STA}	36.64	29.27	68.06	59.78
MMN _{ActivityNet}	32.39	25.04	66.84	55.03
RMMN _{ActivityNet}	39.25	29.59	71.54	60.02

Table 2: MVMR Experiments with Video Retrieval.

7 Conclusion

In this paper, we propose the Massive Videos Moment Retrieval (MVMR) task, which aims to detect a moment for a natural language query from a massive video set. To stimulate the research, we propose a novel method to construct reliable MVMR datasets and build three MVMR datasets using existing NLVL datasets. We further introduce a robust training method called Reliable Mutual Matching to effectively distinguish positives from negative distractors when solving MVMR task.

A Datasets Details

Charades-STA is an extended dataset of action recognition and localization dataset Charades (Sigurdsson et al. 2016) by (Gao et al. 2017) for video moment retrieval. It is comprised of 5,338 videos and 12,408 query-moment pairs in the training set, and 1,334 videos and 3,720 query-moment pairs in the test set. We report evaluation results on test set in our experiments.

ActivityNet-Captions is constructed on ActivityNet v1.3 dataset (Heilbron et al. 2015), where included videos cover various complex human actions. It is originally designed for video captioning, and recently used into video moment retrieval. It contains 37,417, 17,505, and 17,031 query-moment pairs for training, validation, and testing respectively. We report the evaluation result on val_2 set following the setting of the MMN paper (Wang et al. 2022).

TACoS includes 127 videos selected from the MPII-Cooking dataset. It consists of 18,818 query-moment pairs of various cooking activities in the kitchen annotated by (Regneri et al. 2013). It (Gao et al. 2017) consists of 10,146, 4,589, and 4,083 query-moment pairs for training, validation and testing, respectively. We report evaluation results on test set in our experiments.

B Datasets Statistic

We construct three MVMR datasets using existing NLVL datasets (Charades-STA, ActivityNet, and TACoS). The statistic of our constructed MVMR dataset is shown in Table 3.

C Analysis on Filter Methods

We construct reliable MVMR datasets using SimCSE and EMScore. The visualizations of the similarity scores derived by SimCSE and EMScore is shown as Figure 6. For the SimCSE distribution, we select target queries of "person turn a light on", "The person peels a kiwi", and "He is using a push mower to mow the grass" for the Charades-STA, TACoS, and ActivityNet, respectively. The similar queries for those target queries filtered using SimCSE is as Table 4.

D Implementation Details

We use standard off-the-shelf video feature extractors without any fine-tuning. We use VGG (Simonyan and Zisserman 2015) feature for Charades-STA and C3D (Tran et al. 2015) feature for ActivityNet and TACoS following the previous work (Wang et al. 2022). We train RMMN and MMN on 1 NVIDIA RTX A6000 GPU and early stop by averaging scores of all evaluation metrics.

RMMN Our convolution network for deriving 2D feature is exactly same as MMN, including the number of sampled clips N , number of 2D conv layers L , kernel size and channels. We set the dimension of the joint feature visual-text space $d = 256$, and temperatures $\tau_m = \tau_q = 0.1$. We utilize the pre-trained HuggingFace implementation of DistilBERT (Wolf et al. 2019). We set margin ψ as 0.4, 0.3,

and 0.1 for Charades-STA, ActivityNet, and TACoS, respectively. We use AdamW (Loshchilov and Hutter 2017) optimizer with learning rate of 1×10^{-4} , 8×10^{-4} , 1.5×10^{-3} for Charades-STA, ActivityNet, and TACoS, respectively. We set λ as 0.05 for Charades-STA and TACoS and 0.1 for ActivityNet. We set the reliable true-negatives filtering threshold $t_{tr} = 0.9$. We set the number of hard-negative samples to calculate $p'(q|v)$ as 100, 200, and 100 and $p'(v|q)$ as 50, 100, and 5 for Charades-STA, ActivityNet, and TACoS, respectively.

MMN (Wang et al. 2022) adopts a dual-modal encoding design to get video clip and text representations. We utilized the publicly deployed code¹ to implement our own MMN model for our experiment using exactly same hyperparameters setting.

Cross-Encoder Transformer (CET) is a cross-modal encoding model implemented based on 6-layered transformer architecture. It is designed to predict the start and end points of a video moment by utilizing a model architecture which is used in the QA task. We concatenate the pre-extracted video clip features and the text features derived from the DistilBERT to use as an input of the transformer. To concatenate two extracted features, we should equalize the dimensions of two features with a linear layer as follows:

$$\begin{aligned}\bar{H}^v &= H^v W^v \\ \bar{H}^q &= H^q W^q\end{aligned}\quad (11)$$

where $H^v \in \mathbb{R}^{l_v, d^v}$, $H^q \in \mathbb{R}^{l_q, d^q}$, $W^v \in \mathbb{R}^{d^v, d}$, $W^q \in \mathbb{R}^{d^q, d}$. H^v is the pre-extracted video clip features and H^q is the features extracted using DistilBERT. And then, we derive the representation of each video clip feature from the last layer of the transformer-encoder as follows:

$$H^{v,q} = \text{TransformerEnc}(\bar{H}^v \oplus \bar{H}^q) \quad (12)$$

where $H^{v,q} \in \mathbb{R}^{l_{vq}, d}$, $l_{vq} = l_v + l_q$. We utilize only the representation part of video features and they are followed by the 3-layered MLPs and Sigmoid to predict the start and end positions of moment, respectively, as follows:

$$\begin{aligned}p^s &= \text{Sigmoid}(\text{MLP}_s(H^{v,q}_{1:l_v})) \\ p^e &= \text{Sigmoid}(\text{MLP}_e(H^{v,q}_{1:l_v}))\end{aligned}\quad (13)$$

where p^s and $p^e \in \mathbb{R}^{l_v}$. We also introduce the interpolation labels y_i^s, y_i^e to utilize abundant information of moment labels as follows:

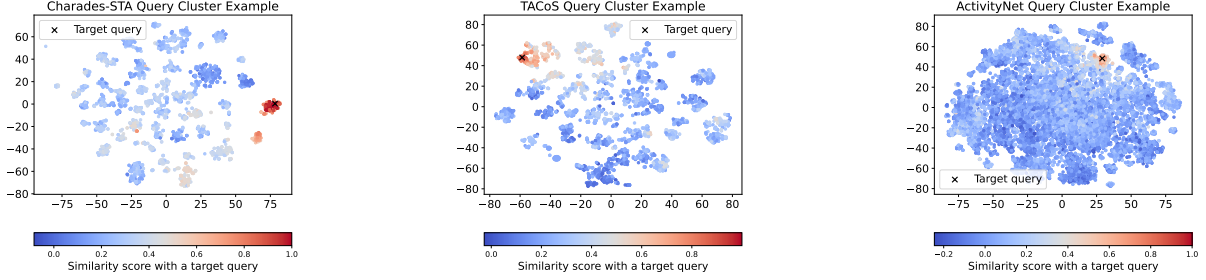
$$\begin{aligned}y_i^s &= \begin{cases} (\frac{x_e - i}{x_e^* - x_s^* + 1})^k & \text{if } x_s^* \leq i \leq x_e^* \\ 0 & \text{otherwise} \end{cases} \\ y_i^e &= \begin{cases} (\frac{i - x_s}{x_e^* - x_s^* + 1})^k & \text{if } x_s^* \leq i \leq x_e^* \\ 0 & \text{otherwise} \end{cases}\end{aligned}\quad (14)$$

We finally use the binary cross-entropy to calculate a loss for the pair of (p_i^s, y_i^s) and (p_i^e, y_i^e) as follows:

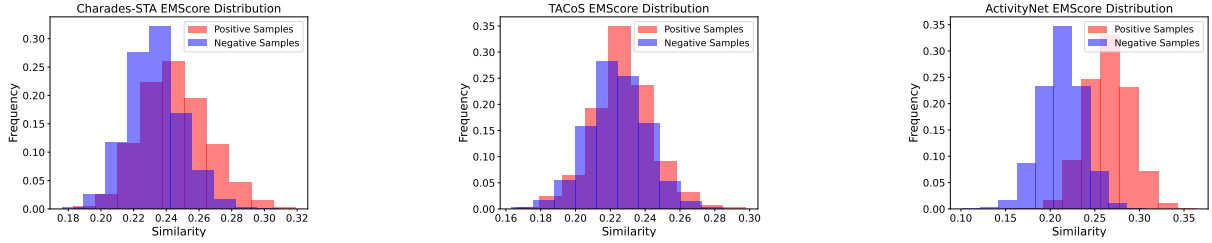
¹<https://github.com/MCG-NJU/MMN>

Dataset	#Queries/#Videos	Avg Len (sec) Moment/Video	Avg #Moments per Query	Avg Query Len	#Retrieval Pool	#Max Positive Moments per Query
MVMR _{Charades-STA}	3716 / 1334	7.83 / 29.48	3.07	6.23	50	5
MVMR _{ActivityNet}	16941 / 4885	40.32 / 118.20	1.11	12.03	50	5
MVMR _{TACoS}	2055 / 25	28.55 / 367.15	2.24	7.31	5	5

Table 3: Summary of datasets



(a) SimCSE Distribution



(b) EMScore Distribution

Figure 6: The Visualization of the SimCSE and EMScore Similarity Distribution

$$\begin{aligned}\mathcal{L}^s &= BCE(p^s, y^s) \\ \mathcal{L}^e &= BCE(p^e, y^e)\end{aligned}\quad (15)$$

where BCE means the binary cross-entropy. The final loss to train the CET model is defined as follows:

$$\mathcal{L} = \frac{\mathcal{L}^s + \mathcal{L}^e}{2} \quad (16)$$

We use $k = 10$ and $d = 512$ as a hyperparameter and AdamW optimizer with learning rate $1e-3$.

Bi-Encoder Transformer (BET) is a dual-modal encoding model which encodes text and video clip features independently. The pre-extracted video clip features are encoded using 6-layered transformer and text features are encoded using the Distil-BERT followed by average-pooling function and 3-layered MLPs.

$$\tilde{H}^v = TransformerEnc(\bar{H}^v) \quad (17)$$

$$\begin{aligned}\tilde{H}^s &= MLP_s(Pool(\bar{H}^q)) \\ \tilde{H}^e &= MLP_e(Pool(\bar{H}^q))\end{aligned}\quad (18)$$

Where $\tilde{H}^v \in \mathbb{R}^d$, $\tilde{H}^s \in \mathbb{R}^d$ and $\tilde{H}^e \in \mathbb{R}^d$. *Pool* means the average-pooling. We calculate the cosine similarity between the encoded video clip representations and the encoded start and end representations to predict a moment.

$$\begin{aligned}p^s &= Sigmoid(r * cosine(\tilde{H}^v, \tilde{H}^s)) \\ p^e &= Sigmoid(r * cosine(\tilde{H}^v, \tilde{H}^e))\end{aligned}\quad (19)$$

We use the interpolation labels and the binary cross-entropy loss for the BET, similar to CET. We use $r = 10$ and $d = 512$ as a hyperparameter and AdamW optimizer with learning rate $1e-3$.

E Examples of False Negative Videos

Illustrative instances of constructed MVMR datasets can be found in Figure 7. This figure shows video instances that have been identified as similar to a specific target query. The target queries correspond to queries of Charades-STA, ActivityNet, and TACoS datasets, sequentially.

Target query: **person opens a fridge door**

NL9AW



OQ54Y



XQVXF



Target query: **He is using a push mower to mow the grass**

v_4JnXF13ktSs



v_Sjx7K9Ybx9Q



v_rMWCaPh9UqE

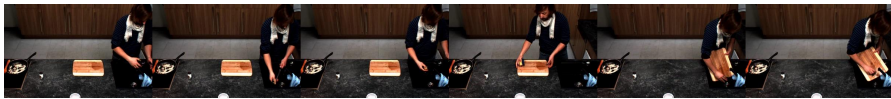


Target query: **The person rinses the knife and cutting board**

s32-d52.avi



s28-d27.avi



s30-d41.avi



Figure 7: Examples of false-negative (positive) videos derived using our methods. Each query corresponds to that of Charades-STA, ActivityNet, and TACoS, sequentially.

Dataset	Target Query	Similar Query Examples (SimCSE)
MVMR _{Charades-STA}	person turn a light on.	person turns on the light. person turns on a lightswitch. a person turns on some lights. person flicks the light switch on. person turned on the light.
MVMR _{ActivityNet}	He is using a push mower to mow the grass.	A man is pushing a lawn mower through the grass. He is pushing a lawn mower to mow the grass. A person is pushing a lawn mower through the grass. A man is pushing a lawn mower through the grass. A person is seen pushing a lawn mower across the yard.
MVMR _{TACoS}	The person peels a kiwi	The person peels one kiwi with a knife. The person peels one kiwi. The person peels one of the kiwi halves. The person peels the kiwi with the fruit peeler. The person peels the kiwi from top to bottom

Table 4: The Similar Query Examples Derived using SimCSE

Name.

Start.

Is there any moment in the video that matches the text?

Yes

If it exists, enter the moment. Leave blank if it does not exist. (Example) in the case of 3 seconds, input 3

Submit.

Next Task (->)

Previous Task (-<)

Enter the task number you want to move. (Ex) in the case of task 3, input 3.

Move.

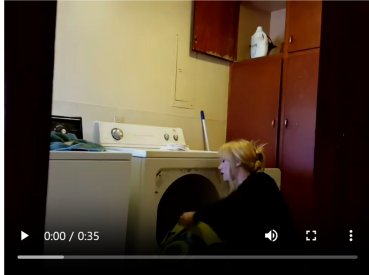
<Video-text matching Human Evaluation>

Login: yny

1. Task ID: 8

2. Text: person puts on shoes.

3. Video ID: J1MMG



0:00 / 0:35

Figure 8: Human Evaluation Sheet Example.

F Human Evaluation for the constructed MVMR Datasets

We conduct a human evaluation on our constructed MVMR datasets to reveal that our method construct MVMR datasets effectively. We recruit crowd workers fluent in English through the university’s online community. The recruited annotators were provided with a detailed description of task definitions, instructions. An example of a sheet we use to conduct a human evaluation is shown in Figure 8.

References

- Anne Hendricks, L.; Wang, O.; Shechtman, E.; Sivic, J.; Darrell, T.; and Russell, B. 2017. Localizing moments in video with natural language. In *Proceedings of the IEEE international conference on computer vision*, 5803–5812.
- Chen, T.; Kornblith, S.; Norouzi, M.; and Hinton, G. 2020. A Simple Framework for Contrastive Learning of Visual Representations. arXiv:2002.05709.
- Dong, J.; Chen, X.; Zhang, M.; Yang, X.; Chen, S.; Li, X.; and Wang, X. 2022. Partially Relevant Video Retrieval. In *Proceedings of the 30th ACM International Conference on Multimedia*, 246–257.

- Escorcia, V.; Soldan, M.; Sivic, J.; Ghanem, B.; and Russell, B. 2019. Temporal localization of moments in video collections with natural language.
- Gao, J.; Sun, C.; Yang, Z.; and Nevatia, R. 2017. TALL: Temporal Activity Localization via Language Query. In *IEEE International Conference on Computer Vision, ICCV 2017, Venice, Italy, October 22-29, 2017*, 5277–5285. IEEE Computer Society.
- Gao, J.; and Xu, C. 2021. Fast video moment retrieval. In *Proceedings of the IEEE/CVF International Conference on Computer Vision*, 1523–1532.
- Gao, T.; Yao, X.; and Chen, D. 2021. Simcse: Simple contrastive learning of sentence embeddings. *arXiv preprint arXiv:2104.08821*.
- Gao, T.; Yao, X.; and Chen, D. 2022. SimCSE: Simple Contrastive Learning of Sentence Embeddings. *arXiv:2104.08821*.
- Ghosh, S.; Agarwal, A.; Parekh, Z.; and Hauptmann, A. 2019. ExCL: Extractive Clip Localization Using Natural Language Descriptions. *arXiv:1904.02755*.
- Hadsell, R.; Chopra, S.; and LeCun, Y. 2006. Dimensionality Reduction by Learning an Invariant Mapping. In *2006 IEEE Computer Society Conference on Computer Vision and Pattern Recognition (CVPR'06)*, volume 2, 1735–1742.
- Heilbron, F. C.; Escorcia, V.; Ghanem, B.; and Niebles, J. C. 2015. ActivityNet: A large-scale video benchmark for human activity understanding. In *IEEE Conference on Computer Vision and Pattern Recognition, CVPR 2015, Boston, MA, USA, June 7-12, 2015*, 961–970. IEEE Computer Society.
- Joshi, M.; Chen, D.; Liu, Y.; Weld, D. S.; Zettlemoyer, L.; and Levy, O. 2020. SpanBERT: Improving Pre-training by Representing and Predicting Spans. *arXiv:1907.10529*.
- Khosla, P.; Teterwak, P.; Wang, C.; Sarna, A.; Tian, Y.; Isola, P.; Maschinot, A.; Liu, C.; and Krishnan, D. 2021. Supervised Contrastive Learning. *arXiv:2004.11362*.
- Krishna, R.; Hata, K.; Ren, F.; Fei-Fei, L.; and Niebles, J. C. 2017. Dense-Captioning Events in Videos. In *IEEE International Conference on Computer Vision, ICCV 2017, Venice, Italy, October 22-29, 2017*, 706–715. IEEE Computer Society.
- Lee, J.; Sung, M.; Kang, J.; and Chen, D. 2021. Learning Dense Representations of Phrases at Scale. In *Proceedings of the 59th Annual Meeting of the Association for Computational Linguistics and the 11th International Joint Conference on Natural Language Processing (Volume 1: Long Papers)*, 6634–6647. Online: Association for Computational Linguistics.
- Lei, J.; Yu, L.; Berg, T. L.; and Bansal, M. 2020. Tvr: A large-scale dataset for video-subtitle moment retrieval. In *Computer Vision—ECCV 2020: 16th European Conference, Glasgow, UK, August 23–28, 2020, Proceedings, Part XXI 16*, 447–463. Springer.
- Liu, D.; Qu, X.; Dong, J.; Zhou, P.; Cheng, Y.; Wei, W.; Xu, Z.; and Xie, Y. 2021. Context-aware biaffine localizing network for temporal sentence grounding. In *Proceedings of the IEEE/CVF Conference on Computer Vision and Pattern Recognition*, 11235–11244.
- Loshchilov, I.; and Hutter, F. 2017. Decoupled weight decay regularization. *arXiv preprint arXiv:1711.05101*.
- Nan, G.; Qiao, R.; Xiao, Y.; Liu, J.; Leng, S.; Zhang, H.; and Lu, W. 2021. Interventional video grounding with dual contrastive learning. In *Proceedings of the IEEE/CVF conference on computer vision and pattern recognition*, 2765–2775.
- Radford, A.; Kim, J. W.; Hallacy, C.; Ramesh, A.; Goh, G.; Agarwal, S.; Sastry, G.; Askell, A.; Mishkin, P.; Clark, J.; Krueger, G.; and Sutskever, I. 2021. Learning Transferable Visual Models From Natural Language Supervision. *arXiv:2103.00020*.
- Regneri, M.; Rohrbach, M.; Wetzel, D.; Thater, S.; Schiele, B.; and Pinkal, M. 2013. Grounding Action Descriptions in Videos. *Transactions of the Association for Computational Linguistics*, 1: 25–36.
- Rohrbach, M.; Regneri, M.; Andriluka, M.; Amin, S.; Pinkal, M.; and Schiele, B. 2012. Script data for attribute-based recognition of composite activities. In *European conference on computer vision*, 144–157. Springer.
- Sanh, V.; Debut, L.; Chaumond, J.; and Wolf, T. 2019. DistilBERT, a distilled version of BERT: smaller, faster, cheaper and lighter. *arXiv preprint arXiv:1910.01108*.
- Seo, M.; Kembhavi, A.; Farhadi, A.; and Hajishirzi, H. 2018. Bidirectional Attention Flow for Machine Comprehension. *arXiv:1611.01603*.
- Shi, Y.; Yang, X.; Xu, H.; Yuan, C.; Li, B.; Hu, W.; and Zha, Z.-J. 2022. EMScore: Evaluating Video Captioning via Coarse-Grained and Fine-Grained Embedding Matching. In *Proceedings of the IEEE/CVF Conference on Computer Vision and Pattern Recognition*, 17929–17938.
- Sigurdsson, G. A.; Varol, G.; Wang, X.; Farhadi, A.; Laptev, I.; and Gupta, A. 2016. Hollywood in homes: Crowdsourcing data collection for activity understanding. In *European Conference on Computer Vision*, 510–526. Springer.
- Simonyan, K.; and Zisserman, A. 2015. Very Deep Convolutional Networks for Large-Scale Image Recognition. In Bengio, Y.; and LeCun, Y., eds., *3rd International Conference on Learning Representations, ICLR 2015, San Diego, CA, USA, May 7-9, 2015, Conference Track Proceedings*.
- Tran, D.; Bourdev, L. D.; Fergus, R.; Torresani, L.; and Paluri, M. 2015. Learning Spatiotemporal Features with 3D Convolutional Networks. In *2015 IEEE International Conference on Computer Vision, ICCV 2015, Santiago, Chile, December 7-13, 2015*, 4489–4497. IEEE Computer Society.
- Vaswani, A.; Shazeer, N.; Parmar, N.; Uszkoreit, J.; Jones, L.; Gomez, A. N.; Kaiser, L.; and Polosukhin, I. 2017. Attention is All you Need. In Guyon, I.; von Luxburg, U.; Bengio, S.; Wallach, H. M.; Fergus, R.; Vishwanathan, S. V. N.; and Garnett, R., eds., *Advances in Neural Information Processing Systems 30: Annual Conference on Neural Information Processing Systems 2017, December 4-9, 2017, Long Beach, CA, USA*, 5998–6008.
- Wang, S.; and Jiang, J. 2016. Machine Comprehension Using Match-LSTM and Answer Pointer. *arXiv:1608.07905*.

Wang, Z.; Wang, L.; Wu, T.; Li, T.; and Wu, G. 2022. Negative sample matters: A renaissance of metric learning for temporal grounding. In *Proceedings of the AAAI Conference on Artificial Intelligence*, volume 36, 2613–2623.

Wolf, T.; Debut, L.; Sanh, V.; Chaumond, J.; Delangue, C.; Moi, A.; Cistac, P.; Rault, T.; Louf, R.; Funtowicz, M.; et al. 2019. Huggingface’s transformers: State-of-the-art natural language processing. *arXiv preprint arXiv:1910.03771*.

Zhang, H.; Sun, A.; Jing, W.; and Zhou, J. T. 2020a. Span-based localizing network for natural language video localization. *arXiv preprint arXiv:2004.13931*.

Zhang, S.; Peng, H.; Fu, J.; and Luo, J. 2020b. Learning 2D Temporal Adjacent Networks for Moment Localization with Natural Language. In *The Thirty-Fourth AAAI Conference on Artificial Intelligence, AAAI 2020, The Thirty-Second Innovative Applications of Artificial Intelligence Conference, IAAI 2020, The Tenth AAAI Symposium on Educational Advances in Artificial Intelligence, EAAI 2020, New York, NY, USA, February 7-12, 2020*, 12870–12877. AAAI Press.

Zhou, K.; Gong, Y.; Liu, X.; Zhao, W. X.; Shen, Y.; Dong, A.; Lu, J.; Majumder, R.; Wen, J.-R.; Duan, N.; and Chen, W. 2022. SimANS: Simple Ambiguous Negatives Sampling for Dense Text Retrieval. *arXiv:2210.11773*.